Supplementary Material

Mineralogy and physicochemical features of Saharan dust wet deposited in the Iberian Peninsula during an extreme red rain event

Carlos Rodriguez-Navarro, Fulvio di Lorenzo, and Kerstin Elert

Department Dept. Mineralogy and Petrology, University of Granada, Fuentenueva s/n, 18002 Granada, Spain

Correspondence to: Carlos Rodriguez-Navarro (carlosrn@ugr.es)

Content

Supplementary Table S1

Supplementary Figures S1-S6

Table S1. Structural formulae of clay minerals (all analyses) in Saharan dust from TEM-AEM analysis

Illite based on $O_{10}(OH)_2$										
	Si	Al^{IV}	Al^{VI}	Mg	Fe	Sum Oct[1]	K	Ca	Na	Sum Int.[2]
1	3.53	0.47	1.69	0.19	0.14	2.03	0.58	0.00	0.00	0.58
2	3.39	0.61	1.29	0.20	0.60	2.09	0.34	0.11	0.12	0.67
3	3.34	0.66	1.43	0.42	0.32	2.17	0.56	0.00	0.00	0.56
4	3.33	0.67	1.20	0.40	0.43	2.03	0.51	0.00	0.00	0.51
5	3.35	0.65	1.65	0.30	0.22	2.17	0.44	0.00	0.00	0.44
Aver.	3.46	0.54	1.49	0.20	0.37	2.06	0.46	0.06	0.06	0.63
Std.	±0.10	±0.10	±0.28	±0.01	±0.33	±0.04	±0.17	±0.08	±0.08	±0.06
Palygorskite based on $O_{10}OH$										
1	4.41	0.00	0.70	0.54	0.07	1.30	0.00	0.00	0.00	
2	3.85	0.00	0.98	0.34	0.59	1.92	0.12	0.03	0.00	
3	3.95	0.00	0.83	0.73	0.41	1.96	0.05	0.00	0.00	
4	4.11	0.00	0.82	0.57	0.28	1.67	0.05	0.05	0.00	
5	4.25	0.00	0.61	0.80	0.16	1.57	0.07	0.02	0.00	
6	4.22	0.00	0.35	1.33	0.12	1.79	0.07	0.00	0.00	
7	3.94	0.00	0.80	1.00	0.24	2.04	0.05	0.04	0.00	
8	4.22	0.00	0.55	1.34	0.18	2.07	0.00	0.06	0.00	
Aver.	4.12	0.00	0.71	0.83	0.26	1.79	0.05	0.03	0.00	
Std.	±0.19	±0.00	±0.20	±0.37	±0.17	±0.26	±0.04	±0.02	±0.00	
Kaolinite based on $O_5(OH)_4$										
1	2.02	0.00	1.82	0.00	0.15	0.00	0.00	0.00	0.00	
2	2.02	0.00	1.92	0.00	0.03	0.00	0.00	0.03	0.00	
3	2.01	0.00	1.98	0.00	0.02	0.00	0.00	0.00	0.00	
4	1.98	0.00	2.01	0.00	0.02	0.00	0.00	0.00	0.00	
5	2.01	0.00	1.87	0.07	0.06	0.00	0.00	0.01	0.00	
6	1.98	0.00	1.96	0.01	0.06	0.00	0.00	0.00	0.00	
7	2.05	0.00	1.82	0.00	0.88	0.00	0.00	0.00	0.00	
Aver.	2.01	0.00	1.91	0.01	0.06	0.00	0.00	0.01	0.00	
Std.	±0.02	±0.00	±0.08	±0.03	±0.05	±0.00	±0.00	±0.01	±0.00	
Smectite based on $O_{10}(OH)_2$										
1	4.01	0.00	1.54	0.09	0.26	1.89	0.14	0.14	0.00	0.42
2	3.62	0.38	1.21	0.31	0.56	2.08	0.21	0.12	0.00	0.45
3	3.71	0.29	1.32	0.19	0.52	2.03	0.16	0.12	0.00	0.40

4	3.57	0.43	0.93	0.12	0.92	1.97	0.24	0.19	0.00	0.62
5	3.51	0.49	1.59	0.21	0.37	2.16	0.17	0.02	0.00	0.20
6	3.38	0.62	1.64	0.16	0.30	2.09	0.09	0.21	0.00	0.51
7	3.84	0.16	1.51	0.22	0.26	2.00	0.05	0.17	0.00	0.39
8	3.71	0.29	0.91	0.35	0.77	2.03	0.31	0.12	0.00	0.55
9	3.66	0.34	1.57	0.42	0.13	2.12	0.30	0.05	0.00	0.40
10	3.64	0.36	1.51	0.37	0.28	2.16	0.15	0.06	0.00	0.27
11	3.55	0.45	1.82	0.15	0.16	2.13	0.15	0.03	0.00	0.21
Aver.	3.65	0.35	1.41	0.24	0.41	2.06	0.18	0.11	0.00	0.40
Std.	±0.17	±0.17	±0.29	±0.11	±0.25	±0.08	±0.08	±0.06	±0.00	±0.13
Illite-smectite mixed layer based on $O_{10}(OH)_2$										
1	3.42	0.58	1.73	0.25	0.23	2.21	0.11	0.05	0.00	0.21
2	3.25	0.75	1.77	0.26	0.24	2.27	0.14	0.02	0.00	0.18
3	3.65	0.37	1.01	0.89	0.47	2.37	0.11	0.00	0.00	0.11
Aver.	3.43	0.57	1.50	0.47	0.32	2.28	0.12	0.02	0.00	0.17
Std.	±0.19	±0.19	±0.43	±0.37	±0.14	±0.08	±0.02	±0.03	±0.00	±0.05

[1] Sum of octahedral cations

[2] Sum of interlayer charge (M^{+} + M^{2+})

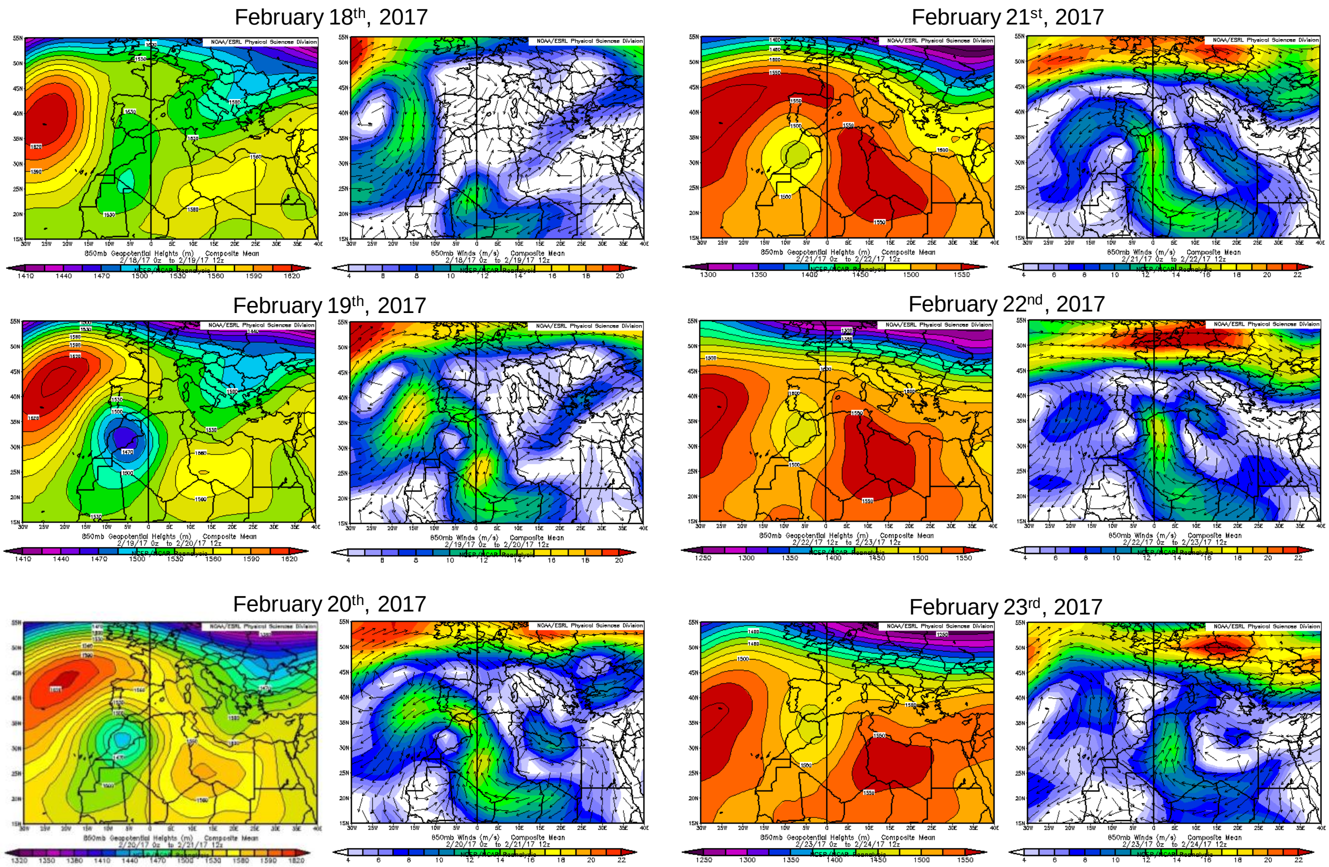

Figure S1. Daily synoptic scale meteorological situation during the days before, during and after the red rain event based on NOAA/ESRL reanalysis for 850 hPa geopotential height. For each date, paired maps of geopotential height and wind field are presented.

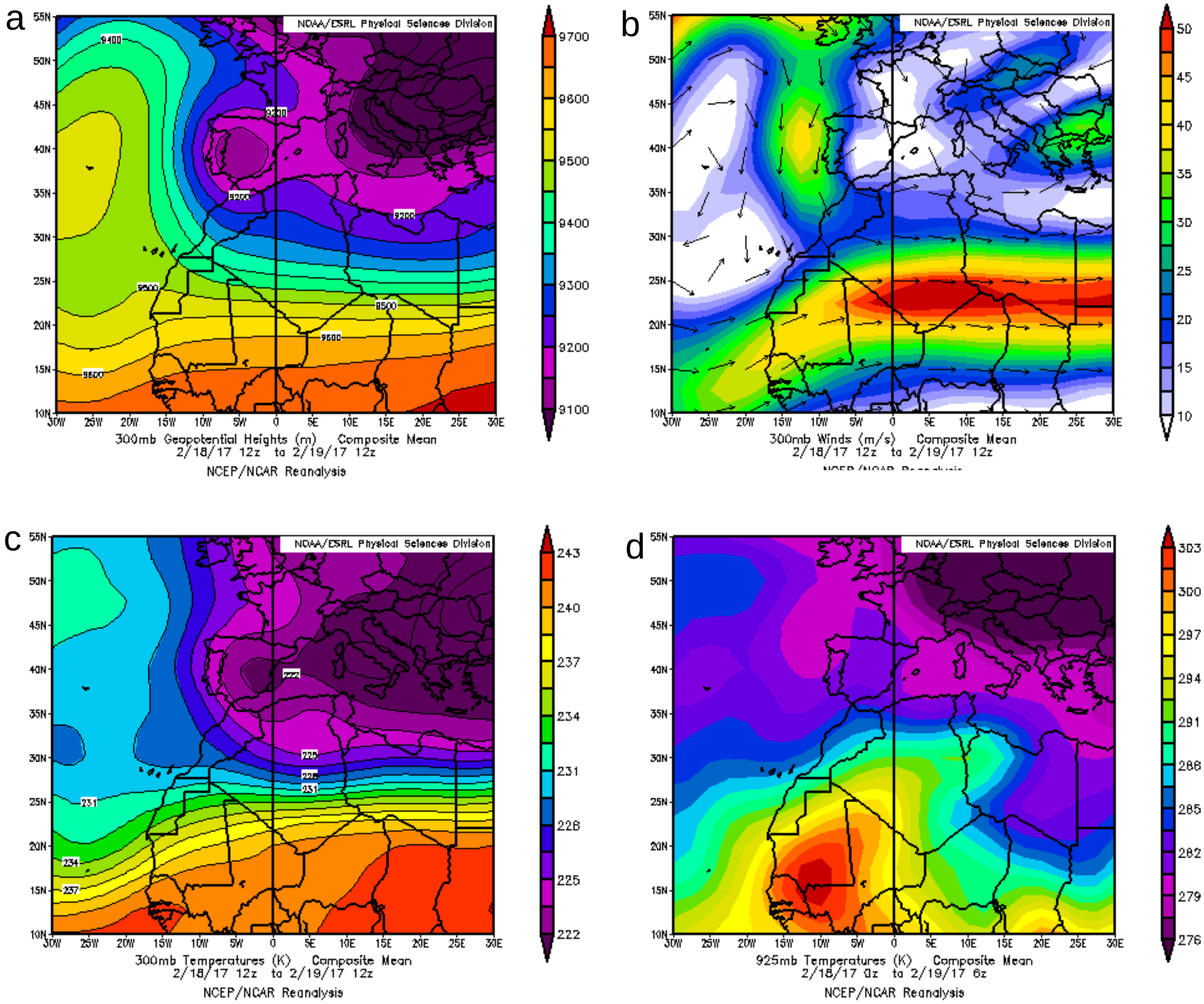

Figure S2. Synoptic scale meteorological situation during the days preceding the development of the north African cyclone responsible for the extreme red rain event (NOAA/ESRL reanalysis). Averaged geopotential heigth (a) and wind field (b), and temperature at 300 hPa (c) and at 925 hPa (d) during February 18-19, 2017.

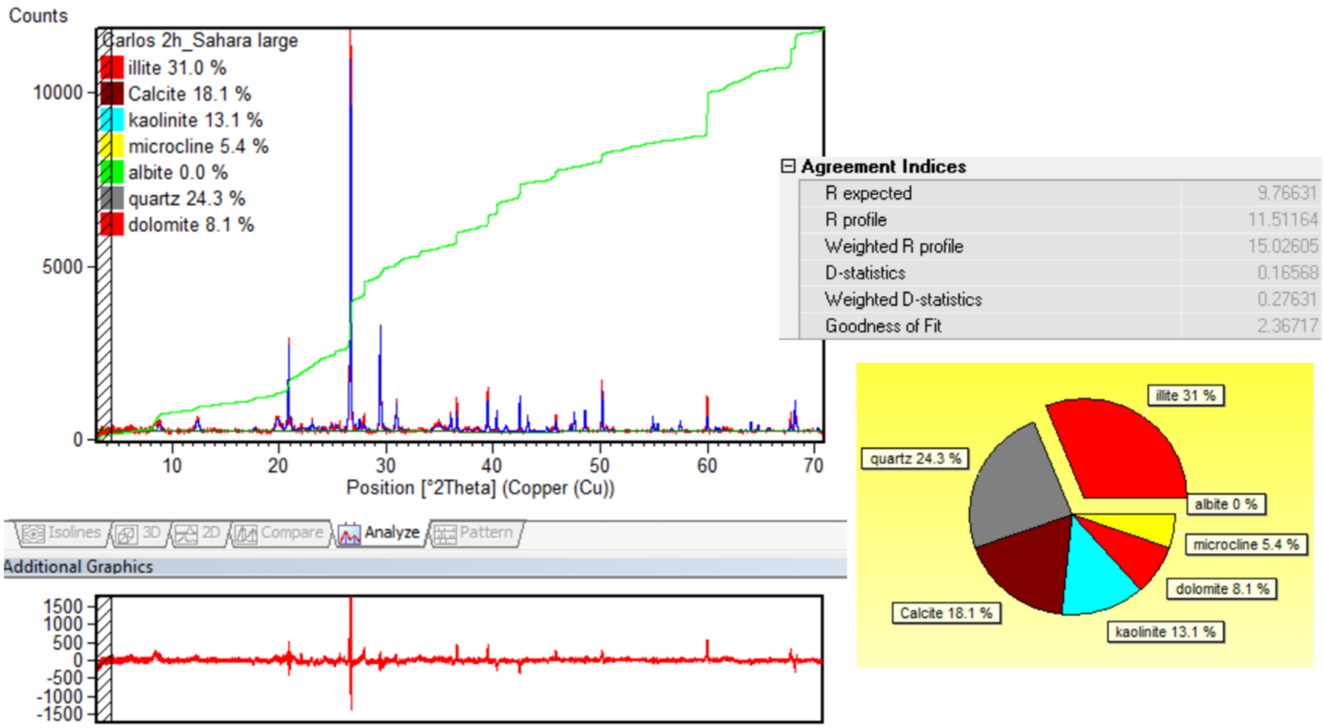

Figure S3. Semiquantitative XRD analysis of a Saharan dust sample collected during the extreme red rain event and performed using the Rietveld full pattern profile method. In addition to the experimental (red) and modeled (bleu) pattern profiles (upper left corner image), the residual curve is shown (lower left) as well as the results of the semiquantitaive analysis (graph on the right).

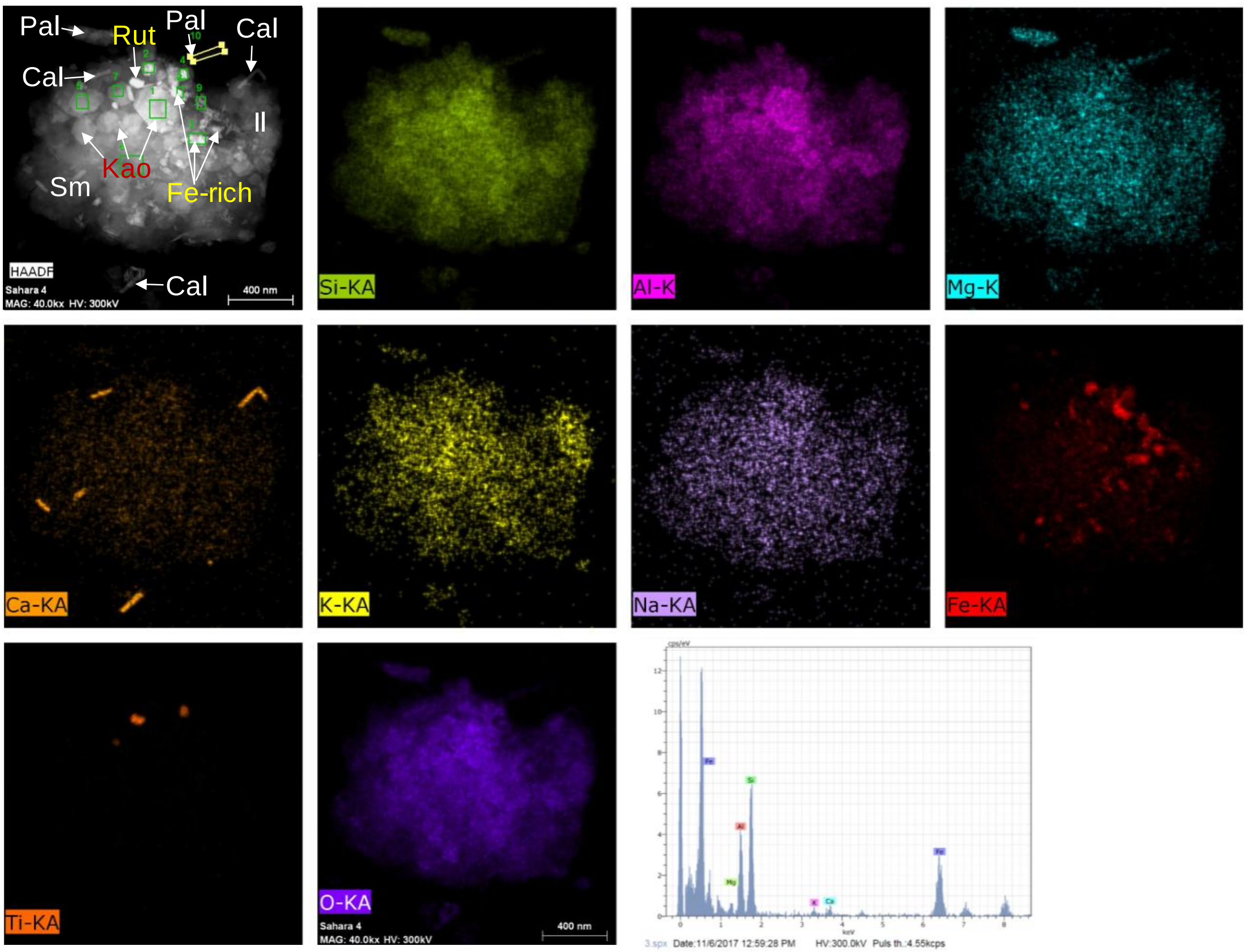

Figure S4. STEM-HAADF photomicrographs and corresponding EDX elemental maps of a clay-rich micrometer-sized aggregate of Saharan dust particles. Based on the compositional analysis, particles of palygorskite (Pal), calcite (Cal), aggregates of iron oxyhydroxide nanoparticle (Fe-rich), rutile (Rut), illite (Il), smectite (Sm), and kaolinite (Kao) were identified. The EDX spectrum corresponds to Fe-rich nanoparticles attached onto the clay minerals (analysis #3 in HAADF image). Note: analyzed spots are outlined with green or yellow (numbered) rectangles in the HAADF image.

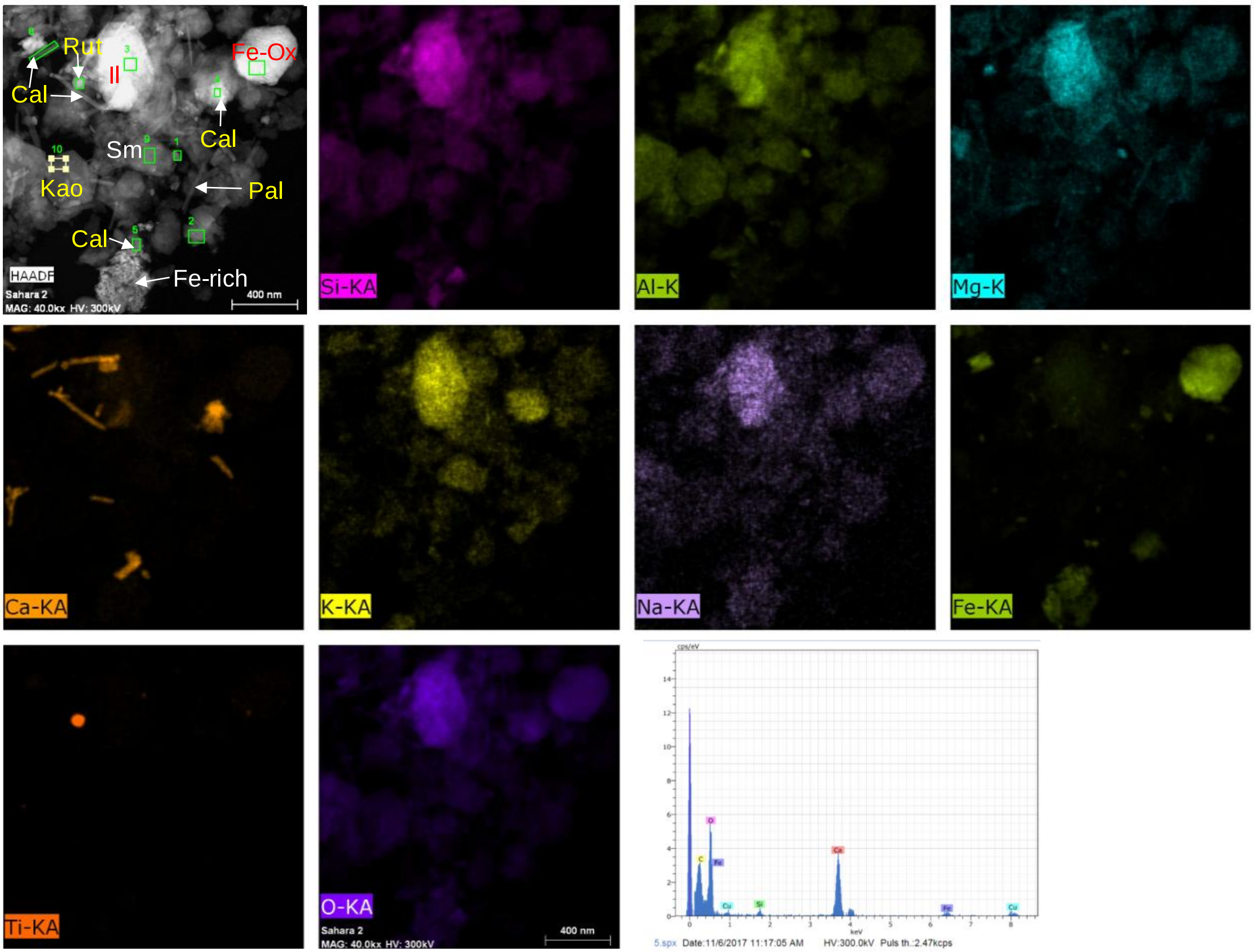

Figure S5. STEM-HAADF photomicrographs and corresponding EDX elemental maps of a micrometer-sized aggregate of Saharan dust particles. Based on the compositional analysis, particles of palygorskite (Pal), calcite (Cal), goethite/hematite (Fe-Ox), aggregates of iron oxyhydroxide nanoparticle (Fe-rich), rutile (Rut), illite (Il), smectite (Sm), and kaolinite (Kao) were identified. The EDX spectrum corresponds to calcite in contact with Fe-rich nanoparticles (analysis #5 in HAADF image). Note the absence of S and N. Note: analyzed spots are outlined with green or white (numbered) rectangles in the HAADF image.

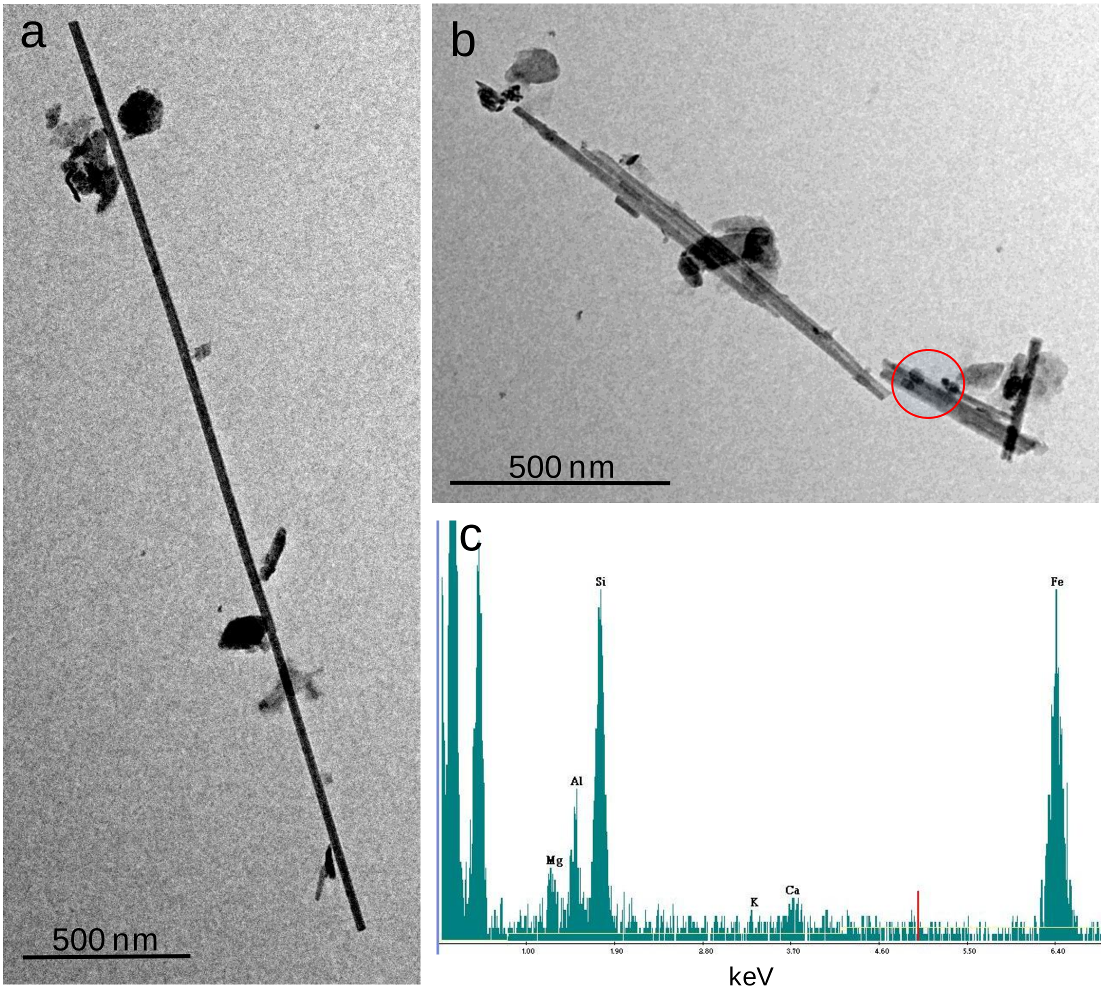

Figure S6. TEM photomicrographs and EDX microanalysis of palygorskite fibers in Saharan dust. a) elongated single fiber of palygorkite with attached aluminosilicate particles (feldspars and clay minerals); b) Palygorskite fibers. The red circle points to Fe-rich (dark) nanoparticles attached to the palygorskite fibers; c) EDX spectrum of the Fe-rich nanoparticles in the circled area of (b). The Mg, Al, and Si (along with small amounts of Ca) correspond to the palygoskite substrate,